Sequence Preference of Mouse H1^0 and H1t[†]

Susan E. Wellman,* Yuguang Song, and Naila M. Mamoon

Department of Pharmacology and Toxicology, 2500 North State Street, University of Mississippi Medical Center, Jackson, Mississippi 39216-4505

Received June 29, 1999; Revised Manuscript Received July 30, 1999

ABSTRACT: Histone H1 proteins bind to DNA and are important in formation and maintenance of chromatin structure. Little is known about differences among variant H1 histones in their interactions with DNA. We examined the effects of histones H1^0 and H1t on thermal denaturation of several DNA species. One of the DNA molecules was a 214-base-pair fragment from the plasmid pBR322, which contains an AT-rich and a GC-rich region. Both H1^0 and H1t bound preferentially to one region of the DNA fragment, a region that is relatively GC-rich. This result indicates that histones H1^0 and H1t are not totally nonspecific but rather bind with some sequence preference to DNA. This conclusion was supported by studies of other DNA species, including two 92-base-pair fragments derived from the two regions of the 214-mer, and several synthetic homocopolymers of DNA. Data obtained with the homocopolymers suggested that the binding preference was not simple preference for GC base pairs. The binding of the two H1 variants was not identical: there appear to be differences in binding site sizes, affinities, and sequence selectivities between H1t and H1^0.

DNA in the eukaryotic nucleus is packaged into highly condensed chromatin. The small, basic core histones are required for assembly of DNA into nucleosomes. In addition to core histones, most eukaryotes have H1 or linker histones, which appear to mediate the condensation of nucleosomes into higher-order structures (reviewed in ref *1*).

The exact nature of the binding of H1 histones to DNA is not known. The H1 histones are highly charged, and their interactions with DNA are presumably primarily (if not completely) electrostatic. This characteristic of the H1 histones as well as their role as packaging proteins has resulted in the inference that they bind to DNA with no sequence specificity. Were this true, then the model of McGhee and von Hippel (*2*) should describe the binding of H1 histones to any sequence of DNA, heterogeneous or homogeneous. In this model for the binding of nonspecific ligands to DNA, the DNA is considered to be an infinite lattice that consists of overlapping sites for ligand.

However, there are data to suggest that histone H1 has some degree of sequence preference, or preference for sequence-dependent structural features (*3*−*12*; reviewed in ref *13*). There are theoretical objections as well to a model of no sequence preference. One is that the H1 histones have some tertiary structure in solution (that of the central globular domain; *14*, *15*), and even the unfolded domains could fold upon binding, using DNA sequences as templates (*16*, *17*). It seems unlikely that distinctive tertiary folds in a protein would bind with equal affinity to any and all sequence-dependent conformations of DNA.

Another reason that the absolutely nonselective model of histone H1 is unsatisfying stems from the existence of isotypes or nonallelic variants of histone H1. There are at least seven of these variants in mammalian cells (*18*). Correlative data have suggested that the variants have different functions; for example, it has been speculated that H1a[1] and H1-1 maintain chromatin in a more open conformation and that H1^0 stabilizes more compact structures (*18*, *20*). Attempts to demonstrate such differences have yielded ambiguous and occasionally contradictory results. It is certainly possible that the variants do not have different functions at all but arise from genes with different regulatory features or are simply redundant. However, recent studies have demonstrated differential effects of particular variants on progression through cell cycle (*21*), replication (*22*), and transcription (*23*), providing strong evidence for functional differences among variants. Even where differences among variants can be unequivocally demonstrated, it is possible that the different effects are a result of varied interactions with other proteins rather than a result of differences in DNA sequence preference or affinities for DNA. Nevertheless, the hypothesis that variants differ in their interactions with DNA remains an attractive one.

Clearly, whether the model of McGhee and von Hippel (*2*) would describe binding of H1 histone to DNA would depend on a number of characteristics of the interaction. A slight preference of the protein for one sequence over another might not be detected in analysis of binding data. On the other hand, if the preference for a specific sequence were great, and the fraction of the DNA lattice that is covered by

[†] This work was supported by MCB-9218440 from the National Science Foundation.

* Corresponding author: telephone (601) 984-1631; facsimile (601) 984-1637; e-mail swellman@pharmacology.umsmed.edu.

[1] The nomenclature used is that proposed in ref *19*. The mouse variant H1c corresponds to H1-1 and the mouse variant H1e corresponds to H1-4.

10.1021/bi9914917 CCC: $18.00
Published on Web 09/17/1999

one protein is reasonably large, then the data would likely not be adequately described by the model.

This paper describes the results of efforts to determine if there are differences among the variant H1 proteins in their affinities for DNA and if there are differences in DNA sequence preference. As an integral part of these efforts, we have evaluated the McGhee−von Hippel model (*2*) for binding of histone H1 variants to DNA, in which the protein ligand binds without sequence preference to the base pairs of the DNA.

We have chosen two histone H1 variants, $H1^0$ and H1t, for study. Both are considered "extreme" variants: their primary sequences are considerably different from those of the somatic variants (*24*). $H1^0$ shows subtle functional differences from somatic variants (*21*−*23*). H1t is a testes-specific variant that is expressed only during spermatogenesis (*25*, *26*). In preliminary studies in our lab, we have also seen rather subtle differences between $H1^0$ and two somatic variants that we have studied, but H1t appeared to behave differently from any of the other variants (data not presented). This was our primary reason for choosing H1t for study. $H1^0$ was chosen because it is not as dramatically different from the somatic variants in function (see above), and of all of the variant proteins that we can produce, it is the easiest to purify in large yield (*27*).

MATERIALS AND METHODS

H1 Histones. The purification of H1 variant histones $H1^0$ and H1t from strains of *Escherichia coli* in which they are inducibly expressed has been described (*27*). Protein concentration was calculated from absorbance in water at 205 nm, using an extinction coefficient of 27.8 or 28 mL mg^{-1} cm^{-1} for $H1^0$ or H1t, respectively, determined as described by Scopes (*28*).

DNA for Thermal Denaturation. Three DNA fragments were synthesized for use in thermal denaturation studies: a 214-base-pair fragment from the plasmid pBR322 (214-mer; *11*) and two fragments that make up 214-mer, the AT-rich 92-base-pair fragment from base pair 4342−4370 (AT-92), and the GC-rich 92-base-pair fragment from base pair 101−192 (GC-92). Each fragment was produced by amplification of the appropriate region, with a thermostable polymerase and buffer conditions suggested by the manufacturer. The primers and the program used to synthesize 214-mer (*29*, *11*) and GC-92 (*17*) have been described. The program used to synthesize AT-92 is the same as that described for AT-122 (*17*), and the primers were 5′-GAGGCCCTTTCGTCTTCAAG-3′ and 5′-GCGATAGCAATTTAACTGTGAT-3′. DNA was dialyzed into BPE buffer, which is 6 mM Na_2HPO_4, 2 mM NaH_2PO_4, and 1 mM EDTA, pH 7.0.

Poly(dA-dT)·poly(dA-dT), poly(dC-dA)·poly(dG-dT), and poly(dG-dA)·poly(dC-dT) were purchased from Pharmacia and were dissolved in and dialyzed against BPE buffer. Mean sizes in base pairs were 5090, 6939, and 1534, respectively.

Thermal Denaturation. The buffer used for all samples was BPE buffer, described above. Thermal denaturation of the DNA fragments was monitored by measuring absorbance at 260 nm in a Cary 3 spectrophotometer. The rate of temperature increase was 1 °C/min. The fraction of DNA strands that was in the coil state at each temperature was calculated from the absorbance data, with straight lines fit to the baseline and to the plateau regions of each curve (*30*). Derivatives of the curves of fraction coil were calculated and smoothed by use of the program Origin (Microcal).

Calculation of Thermal Denaturation Curves. The computer program used to calculate thermal denaturation curves was written by McGhee (*31*). The model used for the DNA−ligand interaction is that described by McGhee and von Hippel (*2*). In this model, the DNA is considered to be an infinite lattice, with overlapping potential sites for ligand binding. McGhee showed that the partition function for DNA in the presence of a specified concentration of ligand could be estimated and used to calculate the fraction of the DNA that was coil at any temperature. Thus parameters that describe the DNA, which would typically be known, and parameters that are thought to describe the ligand−DNA interaction can be used to calculate a thermal denaturation curve, which can be compared to the experimental curve. The parameters that describe the interaction between ligand and double-stranded DNA are n_h, the number of base pairs covered by binding of one ligand; K_h, the intrinsic binding constant; and ΔH_h, the enthalpy of ligand binding. For all calculations, we used a value of 0 for ΔH_h. Including a ΔH term was equivalent to altering the value of K_h (data not shown). For ligands that bind to single-stranded DNA, the parameters n_c, K_c, and ΔH_c describe the interaction. We used a value of 0 for K_c in all calculations. It is possible that the H1 histones have some affinity for single-stranded DNA, but it is clearly weaker than the affinity for double-stranded DNA; incorporating a modest value for K_c (10^5 M^{-1}) into the calculations had the same effect on the curves as choosing a smaller value of K_h (data not shown). The parameters used for the DNA were concentration; T_M, the midpoint of the transition (determined experimentally); ΔH, enthalpy of melting per base pair; and the nucleation parameter σ. Values of ΔH were, for poly(dA-dT)·(dA-dT), 8.35 kcal mol^{-1} bp^{-1}; for poly(dG-dA)·(dC-dT), 8.85 kcal mol^{-1} bp^{-1}; and for poly(dC-dT)·(dG-dA), 8.95 kcal mol^{-1} bp^{-1} (32). ΔH for AT-92 was calculated from the experimental curve, as described (*33*, *34*). Values of σ were varied to obtain calculated curves that corresponded to the experimentally determined ones; for some DNA molecules, a larger value was used at temperatures below the T_M than at temperatures above the T_M. In all cases, use of a larger value of σ for DNA in the presence of protein than for the DNA-only transition resulted in much better correspondence between calculated and experimental curves. Our rationale is this: σ reflects the probability that a single-stranded base is contiguous with a base that is paired (regardless of ligand occupancy). A ligand that binds exclusively to double-stranded DNA, or with much greater affinity than to single-stranded DNA, will alter this probability, for with increasing occupancy of the DNA lattice by ligand, as the temperature increases and unoccupied base pairs melt, the probability that a ligand-bound double-stranded base pair is next to two single-stranded bases will increase.

RESULTS

Binding of $H1^0$ to 214-mer. The DNA fragment 214-mer melts in two distinct phases. At lower temperatures, an AT-rich region of the fragment undergoes denaturation, followed at higher temperatures by melting of a more GC-rich region of the fragment (*11*, *29*). These two distinct transitions allow

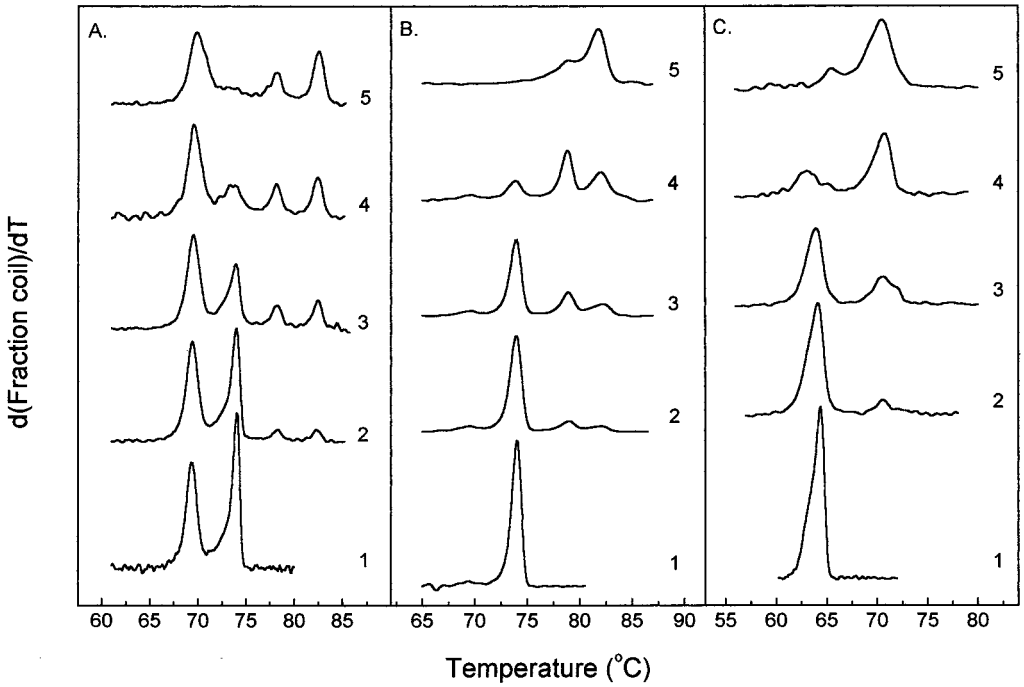

FIGURE 1: Thermal denaturation of 214-mer, GC-92, or AT-92 titrated with $H1^0$. All samples were in 6 mM Na_2HPO_4, 2 mM NaH_2PO_4, and 1 mM EDTA, pH 7. The concentration of 214-mer was 28.9 μM base pairs (135 nM DNA); of GC-92 and AT-92, 29.5 μM base pairs (321 nM DNA). The fraction of bases in the coil conformation at each temperature was calculated from the absorbance data as described in the text. Derivative curves were calculated from curves of fraction coil as a function of temperature and were smoothed. (A) 214-mer and $H1^0$. Curve 1, 214-mer alone; curves 2−5, DNA with protein added at a concentration of (2) 6.75×10^{-8}, (3) 1.35×10^{-7}, (4) 2.03×10^{-7}, or (5) 2.7×10^{-7} M. (B) GC-92 and $H1^0$. Curve 1, GC-92 alone; curves 2−5, DNA with protein added at a concentration of (2) 7.5×10^{-8}, (3) 1.5×10^{-7}, (4) 3.0×10^{-7}, or (5) 6.0×10^{-7} M. (C) AT-92 and $H1^0$. Curve 1, AT-92 alone; curves 2−5, DNA with protein added at a concentration of (2) 7.5×10^{-8}, (3) 1.5×10^{-7}, (4) 3.0×10^{-7}, or (5) 6.0×10^{-7} M.

one to determine whether a ligand binds preferentially to either of the two regions of the DNA. Figure 1 shows the thermal denaturation curves for 214-mer combined with $H1^0$ (panel A). The T_M of the AT-rich region under the conditions used in these binding studies was 69.3 °C, and of the GC-rich region, 73.8 °C. $H1^0$ appeared to bind preferentially to the GC-rich region of the DNA: when the protein was added at concentrations of 67.5 nM (a molar ratio of 1 H1:2 DNA molecules), the melting transition of the AT-rich region changed little from the transition of the DNA alone. In contrast, the fraction of the GC-rich region that was free of protein was decreased. These results indicate that $H1^0$ bound preferentially to sequences within the GC-rich region. At higher concentrations, the fraction of the AT-rich region that was free also showed a decrease, but at all concentrations the fraction of free AT region was substantially greater than that of free GC region. At the highest concentrations of H1 protein, 270 nM (corresponding to a molar ratio of 2 H1 proteins:DNA molecule), almost none of the GC-rich region remained free of protein, but most of the AT-rich region was still free. Two transitions appeared with the addition of protein and increased with increasing concentrations of protein. These are due to the melting of DNA with protein bound. Possibly the two transitions result from melting of DNA with one protein or two proteins bound, but the stoichiometry of these complexes cannot be determined from these data alone. The results of binding H1-4 to 214-mer were qualitatively similar (*11*).

Binding of $H1^0$ to GC-92 and AT-92. We used the GC-rich 92-base-pair fragment and a 92-base-pair fragment from the AT-rich region individually in studies with $H1^0$ (Figure 1B,C). Were the observed preference for the GC-rich region in 214-mer due to simple preference for GC base pairs, then the interaction should be described by the McGhee−von Hippel model (*2*), and it should be possible to calculate thermal denaturation curves (*31*) with the appropriate choices for K and n that correspond to the experimental ones.

The thermal denaturation curves of GC-92 in the presence of $H1^0$ (Figure 1B) were not the biphasic melting curves predicted by use of the McGhee−von Hippel model. Rather, the curves suggest that the proteins bind to discrete sites within the fragment. As is true for the 214-mer studies, the stoichiometry of binding cannot be determined from these data alone. However, the two transitions that appeared could be due to denaturation of DNA with one or two proteins bound. These data would suggest that two proteins can bind per 92 base pairs, or one protein per 46 base pairs. Results obtained with a 122-base-pair fragment suggested that three proteins could bind per 122 base pairs, or one per 40 base pairs (data not shown). The thermal denaturation curves of AT-92 in the presence of $H1^0$, however, were different. In the presence of this protein variant, one rather than two transitions appeared (Figure 1C). Such biphasic curves are predicted by the McGhee model (*31*). Accordingly, the program of McGhee was used to calculate the curves shown in Figure 2, with values for binding site size (n_h) of 40 base pairs and for the binding constant (K_h) of 10^{10} M^{-1}. We had considered the possibility that rather than binding preferentially to particular sequences, the $H1^0$ was binding preferentially to the ends of the molecule. If the binding site size were about 40 base pairs, and if the $H1^0$ were to bind preferentially to DNA ends, then the melting profile should be similar to what we had observed for GC-92 bound to $H1^0$. In this case, however, the melting profile for AT-92 bound

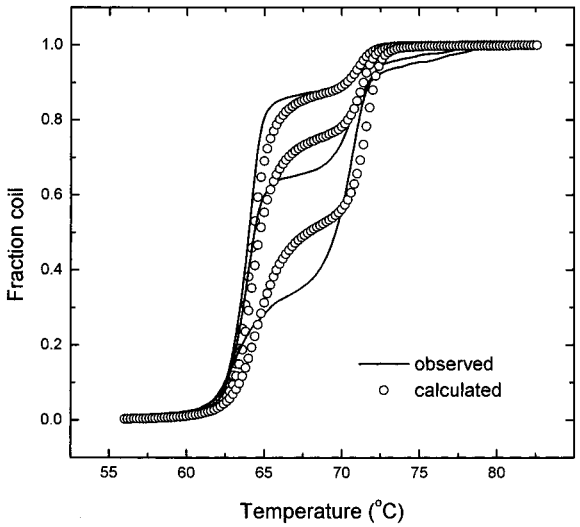

FIGURE 2: Calculated thermal denaturation curves for AT-92 titrated with $H1^0$. The data shown in Figure 1C as derivative curves are shown as fraction of bases in the coil conformation at each temperature, indicated by solid lines. Thermal denaturation curves were calculated as described in the text for $n = 40$ base pairs and $K = 10^{10}$ M^{-1} and are indicated by open circles.

to $H1^0$ should be identical, since AT-92 and GC-92 are the same length. The fact that the profiles are not identical suggests that $H1^0$ does not bind preferentially to DNA ends and thus must bind preferentially to sequences within GC-92 but not within AT-92. The experimental curves for AT-92 bound to $H1^0$ did show substantial differences from calculated curves. The short length of the fragment may contribute to these deviations. In the work of Lifson (*35*), on which McGhee's (*31*) model relies, one of the assumptions necessary for approximating the partition function for a polymer is that for a polymer of very large length, the effects of the ends are negligible; however, AT-92 is short enough that it may not meet this criterion of infinite length, and the effects of the end sequences may not be negligible. The deviations of the calculated from the experimental curves may result in part from the fact that the end sequences are not explicitly treated in the calculations.

We attempted to directly address the question of whether $H1^0$ (and H1t; see below) were binding preferentially to ends of GC-92 rather than to specific sequences within the fragment, by designing it such that it could be ligated together. However, multimers of GC-92 did not have the same pattern of thermal denaturation, one single transition, as did the monomeric form of GC-92. Rather, two transitions were observed for the multimeric form (data not shown).

Binding of H1t to 214-mer. The thermal denaturation curves of 214-mer in the presence of H1t (Figure 3A) were qualitatively similar to those in the presence of $H1^0$, suggesting that H1t also bound preferentially to the GC-rich region of 214-mer.

Binding of H1t to GC-92 and AT-92. Thermal denaturation curves of GC-92 in the presence of H1t (Figure 3B) were qualitatively similar to those in the presence of $H1^0$. Thermal denaturation curves of AT-92 in the presence of H1t (Figure 3C) were unlike those in the presence of $H1^0$ but instead were somewhat like those of GC-92 in the presence of either protein, with two additional transitions appearing. These curves are consistent with binding of H1t to specific sites within both AT-92 and GC-92. However, it is possible that

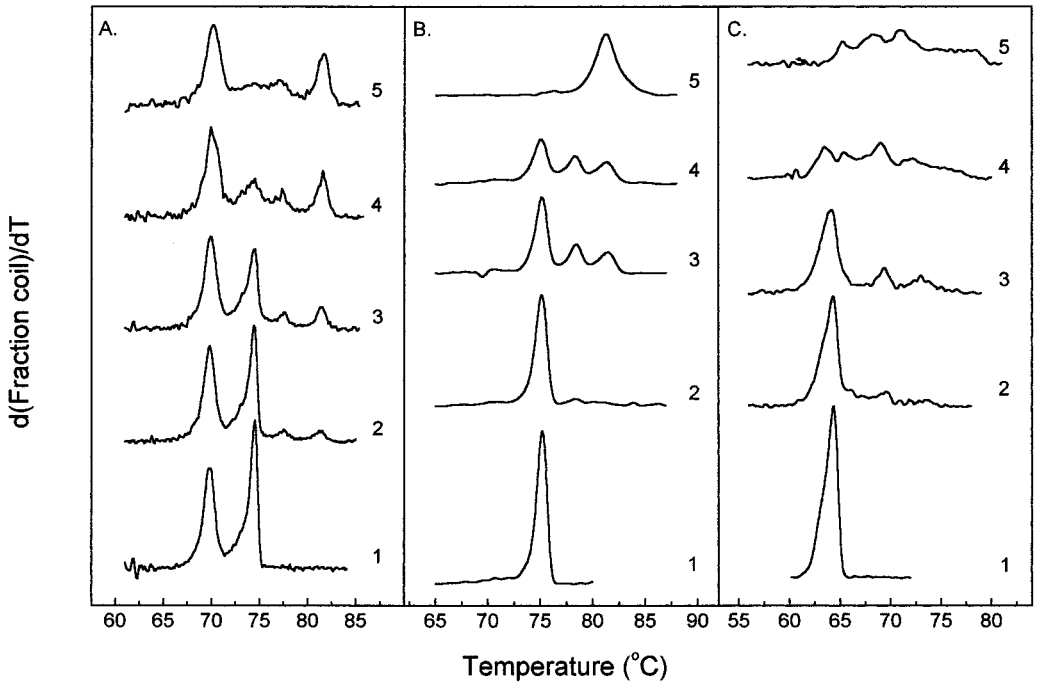

FIGURE 3: Thermal denaturation of 214-mer, GC-92, or AT-92 titrated with H1t. All samples were in 6 mM Na_2HPO_4, 2 mM NaH_2PO_4, and 1 mM EDTA, pH 7. The concentration of 214-mer was 29.2 μM base pairs (136 nM DNA); of GC-92, 29.4 μM base pairs (320 nM DNA); and of AT-92, 29.5 μM base pairs (321 nM DNA). The fraction of bases in the coil conformation at each temperature was calculated from the absorbance data as described in the text. Derivative curves were calculated from curves of fraction coil as a function of temperature and were smoothed. (A) 214-mer and H1t. Curve 1, 214-mer alone; curves 2−5, DNA with protein added at a concentration of (2) 6.75×10^{-8}, (3) 1.35×10^{-7}, (4) 2.03×10^{-7}, or (5) 2.7×10^{-7} M. (B) GC-92 and H1t. Curve 1, GC-92 alone; curves 2−5, DNA with protein added at a concentration of (2) 7.5×10^{-8}, (3) 1.5×10^{-7}, (4) 3.0×10^{-7}, or (5) 6.0×10^{-7} M. (C) AT-92 and H1t. Curve 1, AT-92 alone; curves 2−5, DNA with protein added at a concentration of (2) 7.5×10^{-8}, (3) 1.5×10^{-7}, (4) 3.0×10^{-7}, or (5) 6.0×10^{-7} M.

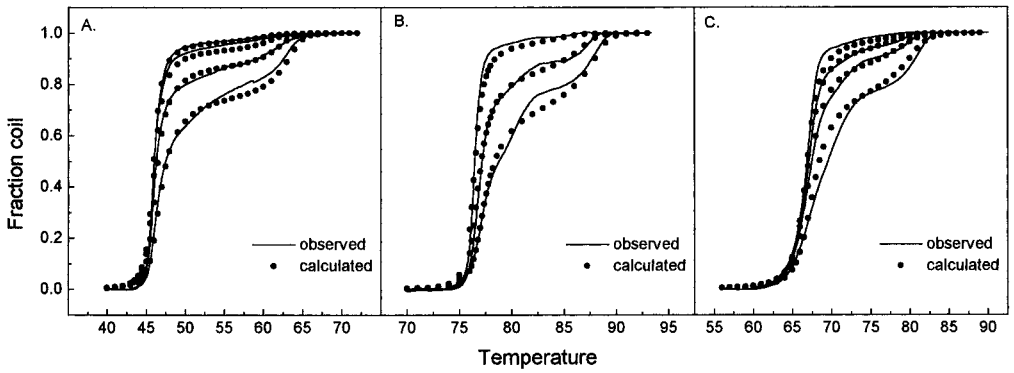

FIGURE 4: Thermal denaturation of poly(dA-dT)·(dA-dT), poly(dC-dA)·(dG-dT) or poly(dG-dA)·(dC-dT) titrated with H1t. (A) Poly(dA-dT)·(dA-dT) and H1t. All samples were in 6 mM Na_2HPO_4, 2 mM NaH_2PO_4, and 1 mM EDTA, pH 7. The concentration of DNA was 31 μM base pairs. Experimental curves, indicated by solid lines, are for DNA with H1t at concentrations, from left to right, of 75, 150, 300, and 600 nM. Calculated curves, indicated by circles, were calculated as described in the text with $n = 11$ base pairs and $K = 2 \times 10^9$ M^{-1}. (B) Poly(dC-dA)·(dG-dT) and H1t. The concentration of DNA was 31.6 μM base pairs. Experimental curves, indicated by solid lines, are for DNA with H1t at concentrations, from left to right, of 75, 300, and 600 nM. Calculated curves, indicated by circles, were calculated as described in the text with $n = 12$ base pairs and $K = 10^8$ M^{-1}. (C) Poly(dG-dA)·(dC-dT) and H1t. The concentration of DNA was 33.6 μM base pairs. Experimental curves, indicated by solid lines, are for DNA with H1t at concentrations, from left to right, of 75, 150, 300, and 600 nM. Calculated curves, indicated by circles, were calculated as described in the text with $n = 10$ base pairs and $K = 10^8$ M^{-1}.

H1t binds preferentially to DNA ends; we cannot eliminate this possibility for H1t as we were able to do for $H1^0$.

Binding of H1t and $H1^0$ to Homocopolymers. To consider the question of simple sequence preference, i.e. AT-rich vs GC-rich, we chose to use homocopolymers of DNA. Because of their simple repeating sequences, we expected their interactions with H1 histones to be described by the McGhee−von Hippel model (*2*). We used the homocopolymers poly(dA-dT)·poly(dA-dT), poly(dG-dA)·poly(dC-dT), and poly(dC-dA)·poly(dG-dT), with the expectation that we would see differences in affinity of the H1 variants for the different polymers. [We could not use poly(dG-dC)·poly(dG-dC) in our thermal denaturation assay because its T_M is too high.]

H1t. For all three homocopolymers bound to H1t, we could calculate curves that closely matched the experimental curves. For poly(dA-dT)·(dA-dT), we used values of 2×10^9 M^{-1} for K and of 11 base pairs for n (Figure 4A). The values used to calculate the curves for poly(dC-dA)·(dG-dT) were $K = 10^8$ M^{-1} and $n = 12$ base pairs (Figure 4B); and for poly(dG-dA)·(dC-dT), $K = 10^8$ M^{-1} and $n = 10$ base pairs (Figure 4C). These curves are calculated, not fitted to the data, and the error in the estimates cannot be estimated; however, the curves were altered in specific and predictable ways by changes in the parameters. For example, Figure 5A shows the same data as in Figure 4A, along with curves calculated with $K = 2 \times 10^9$ M^{-1} and $n = 10$, 11, or 12 base pairs. In Figure 5B, curves have been calculated with $n = 11$ base pairs and $K = 10^9$, 2×10^9, or 5×10^9 M^{-1}. The magnitude of the first transition is affected by the value of n_h, as is the slope of the second transition (Figure 5A; also see Figure 6). The slope of the first transition is slightly sensitive to the value of n_h at very large values, e.g., around 40 (data not shown), and is somewhat sensitive to the value of σ (data not shown). The value of K_h affects the position of the second transition but does not alter the first, and the slope of neither transition is affected (Figure 5B; also see Figure 6). Nonzero values of ΔH and K_c shifted the position of the second transition, that is, the same effect as changing the value of K_h (data not shown). As can be seen, even small changes in n alter the calculated curves; however, considering the possible experimental error, we consider these results to suggest that the binding site sizes for H1t on these three homocopolymers are essentially the same. The affinity of H1t for poly(dA-dT)·poly(dA-dT) appears to be larger than its affinity for the other homocopolymers, by about an order of magnitude.

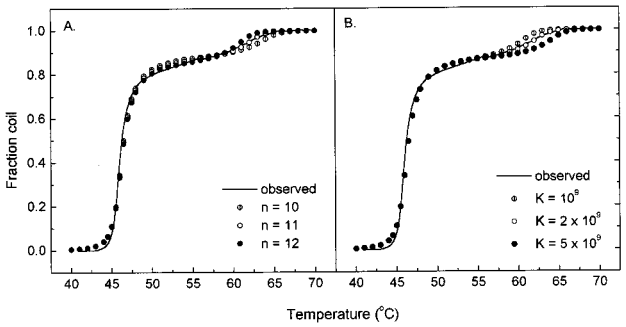

FIGURE 5: Effects on calculated thermal denaturation curves of varying n and K. The data from Figure 4A are plotted (solid line), along with calculated curves (symbols). (A) Curves were calculated for $K = 2 \times 10^9$ M^{-1} and $n = 10$ (circle with bar), 11 (○), or 12 (●) base pairs. (B) Curves were calculated for $n = 11$ base pairs and $K = 10^9$ (circle with bar), 2×10^9 (○), or 5×10^9 M^{-1} (●).

$H1^0$. For poly(dA-dT)·(dA-dT) bound to $H1^0$, several values of K and n were approximately equivalent in generating curves that showed similarities to the experimental curves. These were $K = 10^{15}$ M^{-1}, $n = 30$ base pairs (shown in Figure 6A); $K = 10^{14}$ M^{-1}, $n = 25$ base pairs (Figure 6B); and $K = 10^{13}$ M^{-1}, $n = 20$ base pairs (Figure 6C). The calculated curves showed considerable deviations from the experimental curves, especially those obtained with higher concentrations of protein. The curves calculated for poly(dA-dT)·poly(dA-dT) were shifted, relative to the observed curves, to lower temperature and had steeper slopes for both transitions. Different values of n or K did not improve the correspondence between experimental data and calculated curves for the entire melting curve. The match between experimental and calculated curves was poorer at higher protein concentration; one possibility is that $H1^0$ self-association, which has been reported (*36*), accounts for some of the differences between calculated and observed curves.

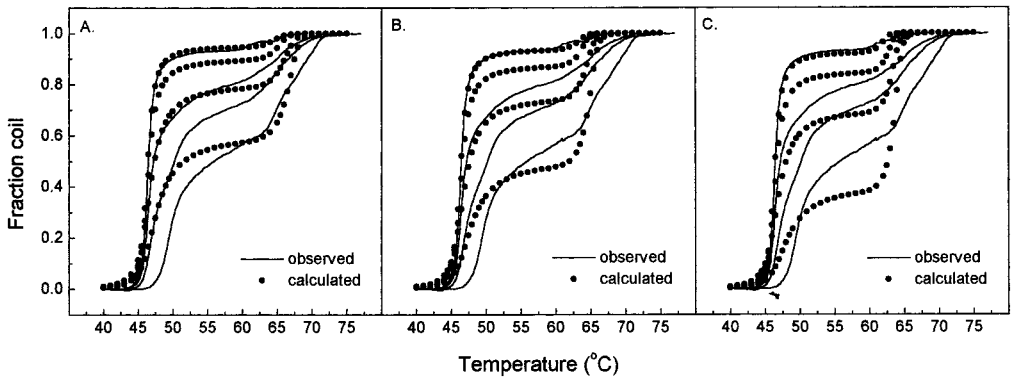

FIGURE 6: Thermal denaturation of poly(dA-dT)·(dA-dT) titrated with $H1^0$. All samples were in 6 mM Na_2HPO_4, 2 mM NaH_2PO_4, and 1 mM EDTA, pH 7. The concentration of DNA was 30.46 μM base pairs. Experimental curves, indicated by solid lines, are, from left to right, for DNA with $H1^0$ at concentrations of 75, 150, 300, and 600 nM. Calculated curves are indicated by solid circles. Curves were calculated as described in the text with (A) $n = 20$ base pairs and $K = 10^{13}$ M^{-1}, (B) $n = 25$ base pairs and $K = 10^{14}$ M^{-1}, or (C) $n = 30$ base pairs and $K = 10^{15}$ M^{-1}.

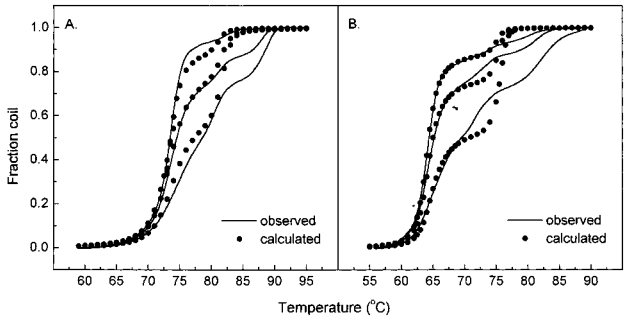

FIGURE 7: Thermal denaturation of poly(dC-dA)·(dG-dT) or poly(dG-dA)·(dC-dT) titrated with $H1^0$. (A) Poly(dC-dA)·(dG-dT) and $H1^0$. All samples were in 6 mM Na_2HPO_4, 2 mM NaH_2PO_4, and 1 mM EDTA, pH 7. The concentration of DNA was 24.8 μM base pairs. Experimental curves, indicated by solid lines, are for DNA with $H1^0$ at concentrations, from left to right, of 75, 150, and 300 nM. Calculated curves, indicated by circles, were calculated as described in the text with $K = 10^{10}$ M^{-1} and $n = 30$ base pairs. (B) Poly(dG-dA)·(dC-dT) and $H1^0$. The concentration of DNA was 20.7 μM base pairs. Experimental curves, indicated by solid lines, are for DNA with $H1^0$ at concentrations, from left to right, of 75, 150, and 300 nM. Calculated curves, indicated by circles, were calculated as described in the text with $K = 10^{12}$ M^{-1} and $n = 30$ base pairs.

For poly(dC-dA)·(dG-dT) and poly(dG-dA)·(dC-dT) bound to $H1^0$, the calculated curves matched the experimental curves quite well at lower temperatures (up to about 80 or 70 °C, respectively; Figure 7). For poly(dC-dA)·(dG-dT), the calculated curves that showed the best correspondence to the experimental curves were those calculated with $K = 10^{10}$ M^{-1} and $n = 30$ base pairs (Figure 7A). For poly(dG-dA)·(dC-dT) bound to $H1^0$, the thermal denaturation curves that showed the best correspondence to the experimental curves were those calculated with $K = 10^{12}$ M^{-1} and $n = 30$ base pairs (Figure 7B). The reasons for the poor correspondence between calculated and observed curves at high temperatures are unknown. In the McGhee model it is assumed that the ligand that is released as the DNA is denatured is capable of binding to DNA that is not yet denatured (*31*). We have preliminary evidence that the structure of $H1^0$ is different at high temperatures than at 25 °C (unpublished data). Possibly at high temperatures $H1^0$ is not capable of binding to DNA in exactly the same manner as at low temperatures, but we have no data to confirm this suggestion.

DISCUSSION

The data together suggest that H1 histones exhibit sequence selectivity in binding to DNA. Such selectivity has been suggested (*3*−*13*), but the reports have not been in agreement. To some extent, the varying selectivities reported have reflected the different assays that have been used in attempts to measure binding. Many assays have been indirect; for example, increased degrees of condensation of DNA have been frequently used as measures of affinity. However, condensation of DNA by H1 histone, while it requires binding of the protein, is the result of numerous processes and could be dictated to a large extent by intrinsic properties of the DNA rather than binding affinity. The data reported here are a more direct assessment of the characteristics of the protein−DNA binding. Another reason for the conflicting reports can be extrapolated from these data; namely, that the interactions are more complicated than may generally be assumed. For example, the results with the heterogeneous DNA fragments seemed consistent with a preference for GC base pairs; however, data on the homocopolymers suggested that both $H1^0$ and H1t bound more tightly to DNA consisting of alternating AT base pairs than to that consisting of alternating GA/CT or CA/GT base pairs. In light of these results, the apparent preference of both proteins for a sequence or sequences within GC-92 cannot simply be due to a preference for GC base pairs. The determinants of sequence preference are not clear from these studies.

The values proposed for the binding site sizes of somatic H1 proteins cover a wide range, from the 15−25 base pairs protected in footprinting experiments (*6*) up to about 80 base pairs, inferred from electron micrographs (*37*); values used in the calculations for $H1^0$, 30−40 base pairs, were within this range. For only one DNA fragment did the value of 40 base pairs result in a reasonably close calculated curve, and that was for AT-92. The value used to approximate the homocopolymer data at lower temperatures was 30 base pairs. This apparent difference may simply be indicative of the error in the determination; alternatively, it may suggest that the precise number of base pairs covered by one protein depends somewhat upon the DNA sequence. The binding site sizes for H1t, 10−12 base pairs, were considerably smaller than those of $H1^0$. There are few data on the H1t variant for comparison to our results, as H1t is not present in most cells. The intrinsic binding constants were also

considerably smaller for this variant. These data suggest that the H1t variant is quite different from $H1^0$, and perhaps from any of the somatic H1 variants. The correspondence between calculated and experimental curves was much better for H1t than for $H1^0$. This may suggest that the McGhee−von Hippel model (*2*) more closely approximates binding of H1t to DNA than that of $H1^0$. Alternatively, we may have failed to find the appropriate combination of terms, including for example cooperativity of binding, binding to single-stranded DNA, or nonzero enthalpy of binding, to precisely describe the binding of $H1^0$ to DNA. Either of these explanations points up, again, that H1t and $H1^0$ differ in the details of their interactions with DNA.

SUMMARY

The model of McGhee and von Hippel (*2*), in which binding sites for a ligand overlap on the DNA lattice, describes the binding of two histone H1 variants, $H1^0$ and H1t, to homocopolymer DNA. Both of these variants appear to bind with higher affinity to poly(dA-dT)·(dA-dT) than to poly(dC-dA)·(dG-dT) or to poly(dG-dA)·(dC-dT). The binding constants are quite large, from 10^8-10^9 M^{-1} for H1t to $10^{10}-10^{15}$ M^{-1} for $H1^0$. The number of base pairs covered by one H1t is 10−12; by one $H1^0$, 30−40. The binding of H1t to either of two heterogeneous fragments of DNA and the binding of $H1^0$ to one of the fragments are not described by the McGhee−von Hippel model. These observations suggest that the H1 proteins have preferred sequences for binding and that the preference is more complicated than simple preference for GC or AT base pairs.

Three of the seven known mammalian H1 variants have been tested and shown to exhibit some degree of sequence preference. These include a representative somatic variant, H1-4 (*11*) and two extreme variants; $H1^0$, which is thought to be associated with inactive chromatin, and H1t, the spermatocyte-specific variant. The intrinsic differences in binding affinity, number of base pairs covered by one protein, and sequence selectivity are likely to be reflected in vivo, in interactions with nucleosomal DNA, and ultimately to result in at least subtle differences in function.

ACKNOWLEDGMENT

We thank Dr. Don Sittman for reading the manuscript and for helpful discussion. We thank Dr. James McGhee, who wrote it, and Dr. Brad Chaires, from whom we obtained it, for the computer program for calculation of thermal denaturation curves.

REFERENCES

1. van Holde, K. E. (1989) *Chromatin*, Springer-Verlag, New York.
2. McGhee, J. D., and von Hippel, P. H. (1974) *J. Mol. Biol. 86*, 469.
3. Šponar, J., and Šormová, Z. (1972) *Eur. J. Biochem. 29*, 99.
4. Hwan, J. C., Leffak, I. M., Li, H. J., Huang, P. C., and Mura, C. (1975) *Biochemistry 14*, 1390.
5. Renz, M., and Day, L. A. (1976) *Biochemistry 15*, 3220.
6. Sevall, J. S. (1988) *Biochemistry 27*, 5038.
7. Izaurralde, E., Käs, E., and Laemmli, U.K. (1989) *J. Mol. Biol. 210*, 573.
8. Suzuki, M. (1989) *EMBO J. 8*, 797.
9. Churchill, M. E. A., and Suzuki, M. (1989) *EMBO J. 8*, 4189.
10. Hendrickson, F. M., and Cole, R. D. (1994) *Biochemistry 33*, 2997.
11. Wellman, S. E., Sittman, D. B., and Chaires, J. B. (1994) *Biochemistry 33*, 384.
12. Yaneva, J., Schroth, G. P., van Holde, K. E., and Zlatanova, J. (1995) *Proc. Natl. Acad. Sci. U.S.A. 92*, 7060.
13. Zlatanova, J., and Yaneva, J. (1991) *DNA Cell Biol. 10*, 239.
14. Clore, G. M., Gronenborn, A. M., Nilges, M., Sukumaran, D. K., and Zarbock, J. (1987) *EMBO J. 6*, 1833.
15. Cerf, C., Lippens, G., Muyldermans, S., Segers, A., Ramakrishnan, V., Wodak, S. J., Hallenga, K., and Wyns, L. (1993) *Biochemistry 32*, 11345.
16. Fasman, G. D., Chou, P. Y., and Adler, A. J. (1976) *Biophys. J. 16*, 1201.
17. Wellman, S. E. (1996) *Biopolymers 39*, 491.
18. Lennox, R. W., and Cohen, L. H. (1984) in *Histone Genes: Structure, Organization, and Regulation* (Stein, G. S., Stein, J. L., and Marzluff, W. F., Eds.) John Wiley and Sons, Inc., New York.
19. Parseghian, M. H., Henschen, A. H., Krieglstein, K. G., and Hamkalo, B. A. (1994) *Protein Sci. 3*, 575.
20. Lennox, R. W. (1984) *J. Biol. Chem.* 259, 669.
21. Brown, D. T., Alexander, B. T., and Sittman, D. B. (1996) *Nucleic Acids Res.* 24, 486.
22. Lu, Z. H., Sittman, D. B., Brown, D. T., Munshi, R., and Leno, G. H. (1997) *J. Cell Sci. 110*, 2745.
23. Brown, D. T., Gunjan, A., Alexander, B. T., and Sittman, D. B.(1997) *Nucleic Acids Res.* 25, 5003.
24. Cole, R. D. (1984) *Anal. Biochem.* 136, 24.
25. Seyedin, S. M., and Kistler, W. S. (1980) *J. Biol. Chem. 255*, 5949.
26. Bucci, L. R., Brock, W. A., and Meistrich, M. L. (1982) *Exp. Cell. Res. 140*, 111.
27. Wellman, S. E., Song, Y., Su, D., and Mamoon, N. M. (1997) *Biotechnol. Appl. Biochem. 26*, 117.
28. Scopes, R. K. (1987) *Protein Purification: Principles and Practice.* Springer-Verlag, New York.
29. Falzon, L., Kirk, C., Chaires, J. B., and Dabrowiak, J. C. (1994) *J. Biochem. Biophys. Methods 29*, 251.
30. Marky, L. A., and Breslauer, K. J. (1987) *Biopolymers 26*, 1601.
31. McGhee, J. D. (1976) *Biopolymers 15*, 1345.
32. Delcourt, S. G., and Blake, R. D. (1991) *J. Biol. Chem. 266*, 15160.
33. Petersheim, M., and Turner, D. H. (1983) *Biochemistry 22*, 256.
34. Puglisi, J. D., and Tinoco, I. (1989) *Methods Enzymol. 180*, 304.
35. Lifson, S. (1964) *J. Chem. Phys. 40*, 3705.
36. Carter, G. J., and van Holde, K. (1998) *Biochemistry 37*, 12477.
37. Clark, D. J., and Thomas, J. O. (1988) *Eur. J. Biochem. 178*, 225.

BI9914917